Contact instability identification by phase shift on C/C friction materials

Alessandro Lazzari, Davide Tonazzi, Jacopo Brunetti, Aurélien Saulot, Francesco Massi

Contact instability identification by phase shift on C/C friction materials

A. Lazzari[ab], D. Tonazzi[a], J. Brunetti[c], A. Saulot[b], F. Massi[a]

[a] Sapienza University of Rome, Department of Mechanical and Aerospace Engineering, Via Eudossiana 18, I-00184, Rome, Italy

[b] Univ Lyon, INSA-Lyon, CNRS UMR5259, LaMCoS, F-69621, France

[c] University of L'Aquila, Department of Industrial and Information Engineering and Economics,Via G. Gronchi 18, I-67100, L'Aquila (AQ), Italy

Abstract

Carbon-carbon (C/C) composite material is currently among the most promising engineering materials for friction applications, where excellent tribological properties, lightweight and good thermal stability are needed. As a result, the industrial demand for C/C composite leads to the need to characterize in detail the frictional and vibrational response of such material, when adopted for high performance braking applications. In this context, the present work shows an experimental and numerical characterization of unstable friction-induced vibrations caused by frictional contact between C/C specimens. The results provide information on the C/C material behavior at high-temperature conditions as well as additional tools to distinguish the occurrence of different vibrational phenomena. The phase shift between vibrational signals has been correlated to different kind of contact instabilities (either mode coupling or negative friction-velocity slope), that can arise and bring to high amplitude oscillations and noise emission. Such correlation has been observed experimentally and reproduced numerically.

Keywords: C/C materials, friction-induced vibrations, phase-shift analysis, mode coupling, friction-velocity slope.

1. Introduction

C/C composite materials consist of carbon fiber reinforcement and a graphite matrix bonding the fibers together. Depending on the reinforcement and matrix processing history, a large variety of C/C materials can be achieved. In particular, in the case of high-performance disc brake systems, the reinforcements are made of carbon fibers resulting from the pyrolysis under a controlled atmosphere of polyacrylonitrile fibers (PAN), the precursor of the process [1-3]. Thanks to their significant operational advantages in braking applications, compared to other traditional friction materials such as steel, C/C composites have seen a relevant increase in commercial demand, over the last few years [4].

The widespread use of these materials, for applications requiring high thermal stability during braking, underlies a strong interest in the study of the tribological and vibrational response of C/C composites over a significantly wide temperature range. In particular, for most industrial and automotive braking applications, is of great importance to understand under which conditions undesired vibrational phenomena, often leading to severe NVH (Noise, Vibration, and Harshness) issues, can arise [5-9].

More in detail, the mutual interaction between the local frictional behavior and the system response can result in self-excited friction-induced oscillations, characterized by an exponential increase of the amplitude of vibration until non-linear contributions limit the further growth of the oscillations [10-12]. In the literature, the onset of the negative friction-velocity slope and the instability is often related to different physiochemical and rheological contributions at the frictional surfaces, as well as wear and structural damage [8, 13]. The occurrence of such unstable friction-induced vibrations is mainly

attributed to two different phenomena: either the mode coupling [11, 14-19] or the negative friction-velocity gradient [20-23]. The onset of a mode-coupling instability is brought about by two modes of a structural system, coupling through the contact forces, and leading to high amplitude oscillations [11, 19, 24-27].

On the other hand, the occurrence of a negative friction-velocity slope instability is caused by an increase of the friction coefficient while the relative sliding velocity decreases, which leads, in turn, to a negative apparent damping in the equations of motion. This phenomenon results in a single structural mode of the system becoming unstable and, therefore, in the occurrence of unstable friction-induced vibrations [28-32]. Moreover, the presence of a negative friction-velocity gradient brings to an apparent negative damping in the equation of motion [33, 34], leading to the exponential increase of the system oscillation. This macroscopic gradient, affecting the dynamic response of the mechanical system, is often associated to the physiochemical and rheological response of the interface with the sliding velocity [29]. The negative friction-velocity slope is also considered as one of the main causes of the stick-slip phenomenon, characterized by alternate phases of sticking and slipping motion, leading to impulsive excitation of the mechanical system [22, 35, 36].

Over the past few years, the dynamic instabilities described above have been the object of several research studies, aimed to provide experimental and numerical approaches intended to characterize and predict the occurrence of these phenomena [37-40]. Recently, Di Bartolomeo et al. [29] investigated experimentally the occurrence of the negative friction-velocity slope instability for C/C materials under different working temperatures, showing the occurrence of unstable vibrations due to the increase of the friction coefficient during braking [41]. Numerically, the occurrence of self-excited friction-induced vibrations has been often studied in literature through minimal numerical models, characterized by two or three degrees of freedom [42-44]. In this regard, Shin et al. [33] proposed a two-degree-of-freedom numerical model, characterized by a linearly decreasing friction coefficient as a function of the relative

velocity (negative friction-velocity gradient) at the contact, in order to study the onset of unstable friction-induced vibrations in presence of a negative apparent damping. Analogously, Hoffmann et al. [45] investigated the mode coupling instability in presence of structural damping, by adopting a minimal single mass two-degree-of-freedom model. In this respect, a consolidated and computationally efficient approach to evaluate the stability of a system is the complex eigenvalue analysis [46-49]. Thanks to this analytic technique, it is possible to study the evolution of the Hopf bifurcation points as a function of the main parameters of the model and predict the occurrence of dynamic instabilities [50].

Despite the number of studies carried out on unstable friction-induced vibrations, in real industrial problems, it is often challenging to determine the nature of the observed dynamic instabilities. Nevertheless, the understanding of the origin of the instability, either mode coupling or negative friction-velocity slope, is fundamental for determining the necessary design improvements to stabilize the system. Within this framework, the goal of this study is to reproduce and investigate the occurrence and the main features of unstable friction-induced vibrations for C/C materials and to provide an additional approach to distinguish dynamic instabilities caused by either mode coupling or negative friction-velocity gradient. First, samples of C/C materials in frictional contact are tested on a suitable tribometer, at different temperature conditions and under well-controlled boundary conditions. The tribological and dynamic response is analyzed and the obtained results are discussed.

Then, the experimental outcomes are numerically reproduced by means of a two-degrees of freedom numerical model, characterized by an oscillator sliding on a belt. Complex eigenvalue analyses and transient simulations have been carried out to identify, as a function of the values and trend of the friction coefficient, the stable and unstable configurations. The numerical results are finally compared with the experimental ones for correlating the phase behavior of the time signals, observed both numerically and experimentally, with the nature of the reproduced contact instability. Lastly, general conclusions are provided.

2. Experimental setup

To study the occurrence of unstable friction-induced vibrations and their correlation with the frictional response of C/C materials, under different operating conditions, a specifically designed tribometer has been used. The experimental test bench allows for the relative motion of two C/C specimens in contact and provides accurate measurement of friction-induced vibrations and contact forces, originated by the frictional interactions between the tested samples. The setup has been developed with a simple dynamics, in order to well distinguish its dynamic response from the dynamics of the contact excitation [51, 52]. Moreover, thanks to the adopted test rig, boundary conditions such as sliding velocity, contact pressure and temperature of the frictional interface can be controlled.

A simplified diagram of the experimental setup, named TriboAir, is shown in Figure 1.

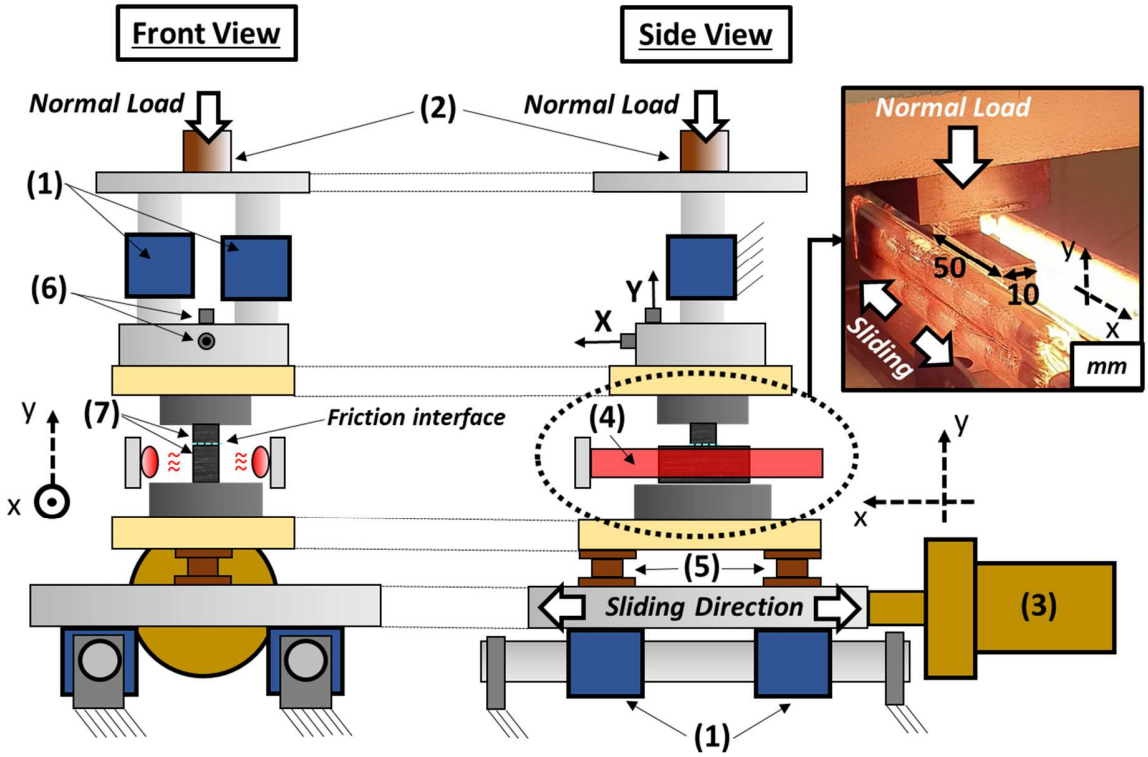

Figure 1. Schematic view of the experimental test bench: (1) Air bearings; (2) Dead weights; (3) Linear voice coil motor; (4) IR lamps; (5) 3-axial force transducers; (6) Accelerometers; (7) C/C material specimens in frictional contact.

High accuracy dynamic measurements are achieved thanks to the air bearings (1), which allow the relative motion of the tested samples without introducing parasitic noise affecting the measure of friction-induced vibrations and contact forces. The air bearing system consists of air guides placed on the upper and lower part of the setup. Four air bearings are assembled at the bottom of the moving base and allow the sliding motion of the lower C/C sample, with respect to the upper one, along the tangential direction. Other two air guides are placed along the normal direction to the contact, allowing the load application through dead weights (2), disposed at the top of the test bench. In order to control the sliding velocity and the law of motion, a linear voice coil motor (BEI KIMCO LA30-75-001A) (3), coupled to a linear

optical encoder with a resolution of 0.1 micrometer, drives the motion of the lower C/C specimen, while the upper C/C sample is kept stationary and in frictional contact with the lower one.

Thanks to the air-bearings and the voice coil motor, the moving part is completely suspended and the only surface in frictional contact is the one under investigation. Parasitic vibrations from other interfaces are then prevented.

The temperature at the contact interface can be controlled by means of two IR lamps (4), placed alongside the tested samples. A specific thermal profile can be achieved thanks to a PID temperature controller (GEFRAN F650). Moreover, a ceramic insulation system has been specifically designed to best convey the heat to the contact samples. Temperature can be monitored thanks to a thermocouple placed inside a hole at 2 mm from the contact interface of the lower C/C sample, to be as close as possible to the contact interface. Regarding the measure of the contact forces, two 3-axial force transducers (KISTLER 9017B) (5) are assembled on the moving base of the tribometer. The vibrational response due to the frictional interaction between the samples in sliding contact is measured by two accelerometers (6), placed in the tangential and normal directions with respect to the contact, on the upper part of the setup.

All data are recorded by an acquisition system SIRIUSi - DEWESOFT, based on DualCoreADC® technology with dual 24-bit delta-sigma analog to digital converter (ADC), with a sampling frequency equal to 200 kHz and then post-processed by *Matlab* ©.

The samples of C/C materials (7) are machined from a real brake disc preliminary tested in a dedicated brake apparatus. As a result, the contact surfaces of the specimens are already subjected to a running-in, aimed to reproduce friction conditions of the tested samples as close as possible to the effective operating ones. The repeatability of the investigated friction evolutions has been obtained on several samples coming from discs made of the same C/C material.

The C/C specimens consist of two blocks of simple geometries. The sample clamped on the mobile base of the test rig is a rectangular prism of 10x50x25 mm (contact surface 10x50 mm), while the sample

clamped on the upper part of the tribometer is a cube of 10 mm side. Each stroke of the lower sample covers a sliding distance of 40 mm.

By testing these samples in the above-described tribometer, a reliable characterization of the frictional and vibrational response can be achieved [29].

3. Experimental analysis

In order to investigate the material behavior of C/C material under different boundary conditions, the frictional and dynamical response of the tested samples has been characterized by defining an experimental test protocol, consisting of different sliding velocities and operational temperatures at the contact interface.

3.1 Experimental campaign protocol

During the frictional contact, the dynamical and tribological behavior of C/C materials is strongly affected by the boundary conditions [29, 53, 54]. As a result, with the purpose of investigating the main features of the C/C material response, a suitable protocol, aimed to study the occurrence of dynamic instabilities, has been defined.

Each test consists of cycles of back-and-forth of the lower sample with respect to the upper one and the experimental protocol is characterized by tests carried out under constant and variable sliding velocity profiles, illustrated in Figure 2.

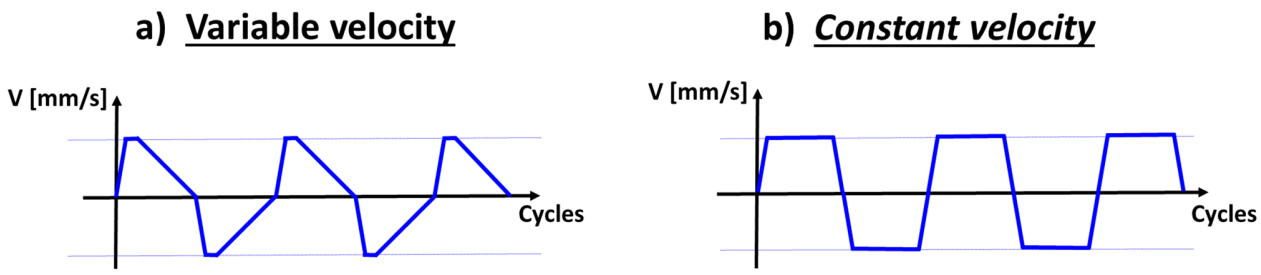

Figure 2. Example of variable and constant velocity profiles during the back-and-forth cycles of the lower C/C specimen: a) Decreasing velocity in each stroke; b) Constant velocity in each stroke.

The variable velocity profile test (Figure 2.a) consists of braking cycles characterized by a sliding velocity varying from 20 mm/s to 0 mm/s, with a deceleration of 6 mm/s^2, in each stroke of the lower sample. This type of test allows simulating braking conditions and retrieving information on the frictional and vibrational material response when using the C/C composites in braking applications. Nevertheless, it should be kept in mind that during tests the decrease of the velocity is imposed by the external motor. In fact, the aim is not to reproduce real braking, but to investigate the evolution of the frictional and dynamic response as a function of the velocity.

On the other hand, tests carried out with a constant velocity profile (Figure 2.b) allow decoupling the velocity variation from the other test parameters. The experimental protocol provides for tests carried out with a constant velocity equal to 15 mm/s and 3 mm/s.

Each test is performed under a normal load of 15 N, held constant thanks to the dead masses, guided by the air bearings on the upper part of the setup. As a result, accounting for a contact surface of 10x10 mm, an average contact pressure of 0.15 MPa is maintained constant throughout the tests. Each measurement is carried out following a specific temperature profile described in Figure 3.

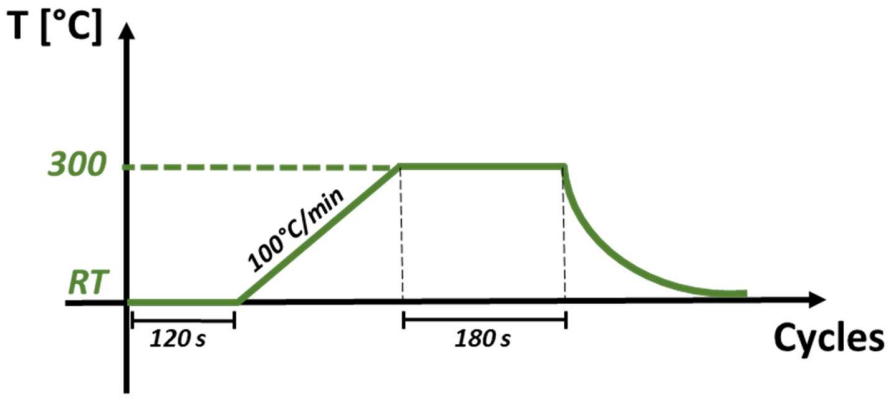

Figure 3. Temperature profile of each experimental test.

After two minutes of sliding cycles at room temperature condition, the IR lamps are turned on and the temperature is linearly increased with a gradient of 100 °C/minute. During the heating process, the tested samples are maintained in contact and in relative sliding condition. Once the contact interface achieves 300 °C, the temperature is kept constant for 3 minutes and both the frictional and vibrational behavior of the tested samples in contact is investigated. After each test, a natural cooling follows.

In general, a variation of temperature, can affect material properties and, consequently, the frictional and dynamic response of the system [55-57]. Nevertheless, it should be remarked that C/C composites are widely known for retaining their thermo-structural properties also for temperatures higher than 1000 °C [3, 4]. However, the tribological response of such materials can be strongly affected even at almost 300 °C [29, 57, 58], which is the maximum temperature at which the analysis is carried out.

Before starting the sequence of the experimental tests, an initial running-in is carried out in order to ensure a well-established contact between the contacting surfaces. It consists of 15 minutes of sliding motion in frictional contact of the tested samples at constant velocity (20 mm/s) and room temperature condition. After the running-in, the sequence of tests presented in Table 1 is carried out.

Test	Velocity [mm/s]	Deceleration [mm/s^2]	Contact pressure [MPa]	Max Temperature [°C]
Variable V	20→0	6	0.15	300
Higher constant V	15	/	0.15	300
Lower constant V	3	/	0.15	300

Table 1. Experimental protocol: sequence of tests carried out for the experimental characterization of the C/C sample frictional behavior.

First, a variable sliding velocity test is performed in order to study the C/C material response in braking conditions. Then, tests carried out at constant sliding velocity, respectively at 15 mm/s and 3 mm/s, follow.

Figure 4 shows, as a reference test, two cycles of back-and-forth at room temperature condition, during the variable sliding velocity test. From the top to the bottom, the signals correspond to the friction coefficient measured during the frictional contact, the vibrational signals on both the tangential and normal direction to the contact, *X* and *Y* respectively, and the velocity profile imposed on the lower moving sample by the linear voice coil. The symmetric reversal of sign of the friction coefficient in each stroke is due to the back-and-forth motion of the lower sample with respect to the upper one.

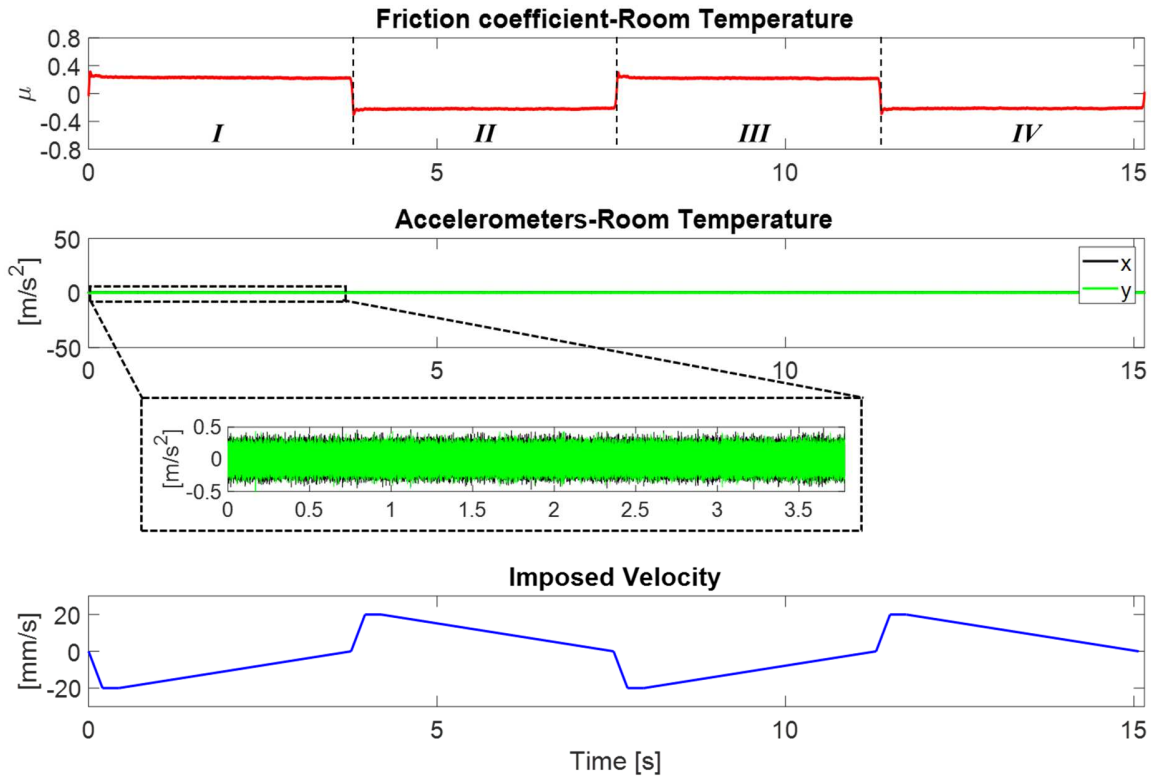

Figure 4. Example of signals recorded during two back-and-forth cycles (four strokes of the lower sample), at room temperature condition (≈25 °C), in the variable sliding velocity test (V=20⟶0 mm/s). From the top: friction coefficient (ratio between tangential and normal force), accelerometer signals along the tangential (X, black) and normal direction (Y, green) to the contact and imposed sliding velocity profile.

As can be noted, at room temperature condition the friction coefficient stays almost constant during each stroke. The vibrational response is characterized in this case by low-amplitude stable friction-induced vibrations, as shown in the inset of Figure 4. The imposed velocity profile is the one already described in Figure 2.a and characterized by a fast acceleration (100 mm/s^2) up to 20 mm/s, to which follows a braking deceleration (6 mm/s^2) covering most of the stroke.

The analysis of the frictional and vibrational response in the different tests provides meaningful information in terms of C/C material behavior and allows studying the onset of the vibrational phenomena.

3.2 Result discussion: Variable velocity test

The variable velocity test has been carried out according to the temperature profile described in Figure 3. While at room temperature condition an almost constant friction coefficient and stable friction-induced vibrations are observed in each stroke (Figure 4), a significantly different scenario is observed at 300 °C. Figure 5 shows the frictional and vibrational response recorded at 300 °C.

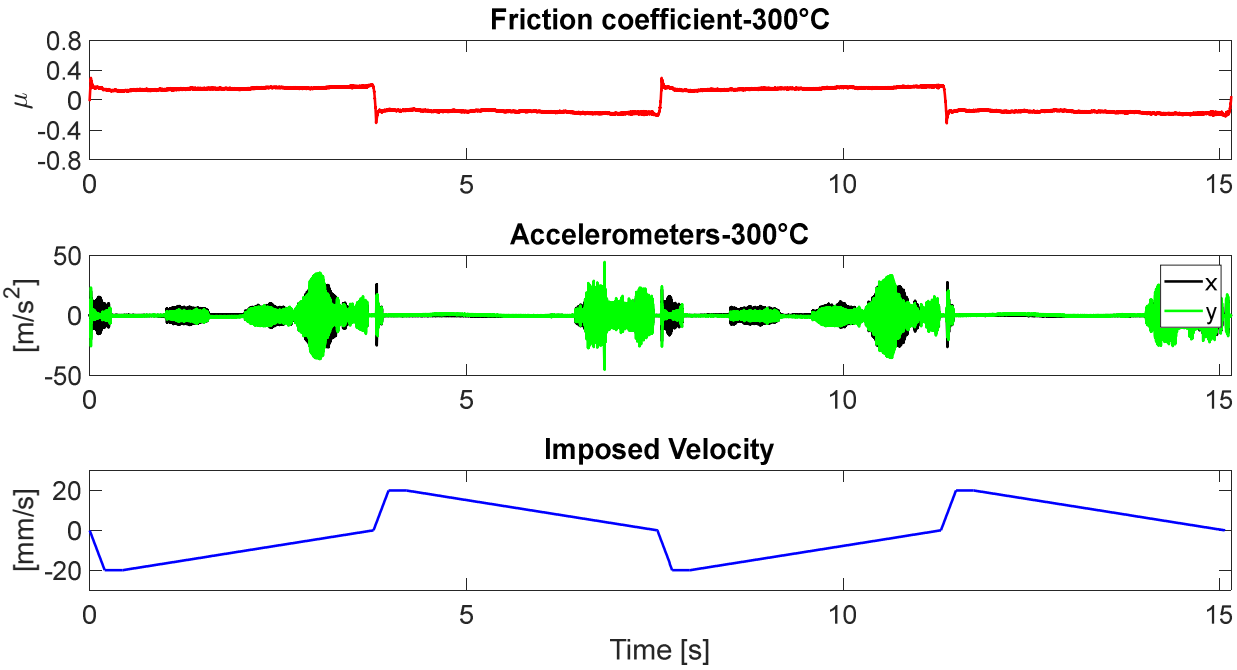

Figure 5. Example of signals recorded during two back-and-forth cycles, at 300 °C, in the variable sliding velocity test (V=20→0 mm/s). From the top: friction coefficient, accelerometer signals along the tangential (X, black) and normal (Y, green) direction to the contact and imposed sliding velocity profile.

Differently from braking carried out at room temperature condition, at 300 °C, an increase of the friction coefficient with the decrease of the sliding velocity can be observed. Moreover, the vibrational response of the C/C specimens is characterized, in this case, by the presence of unstable friction-induced vibrations. Further information can be obtained by analyzing the behavior of the friction coefficient and

the dynamic response during one single stroke. As an example, Figure 6 shows the comparison between the signals (friction coefficient and acceleration along the *X* direction) acquired at room temperature and at 300°C, in the third stroke of Figure 4 and Figure 5, respectively.

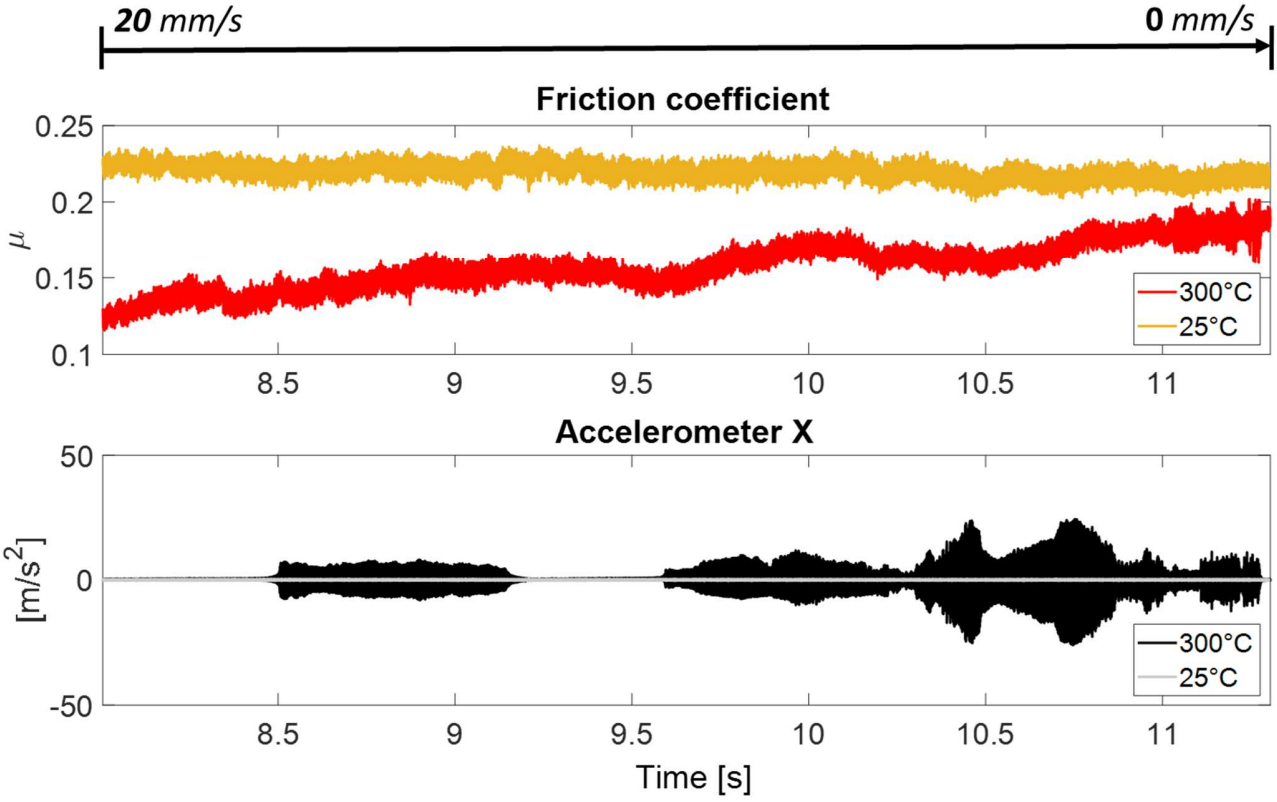

Figure 6. Comparison of the friction coefficient and the vibrational response along the X direction, measured at room temperature and at 300°C (third stroke of Figure 4 and Figure 5, respectively).

It can be noticed that the friction coefficient observed during braking at a higher velocity, at 300 °C, is characterized by a lower value compared to the one at 25 °C. This phenomenon promotes the occurrence of a negative friction-velocity slope toward the end of braking, where a significant increase of the friction coefficient, while lowering the imposed velocity, can be observed. Regarding the vibrational response, the comparison shows a clear difference between the stable response characterizing the material behavior at room temperature condition and the occurrence of dynamic instabilities during braking at 300°C. In

this regard, Figure 7 shows the trend of the friction coefficient during braking and the occurrence of the unstable friction-induced vibrations at 300 °C. From the top, the friction coefficient, the measured accelerations along the *X* and *Y* directions and the spectrogram of the vibrational response along the *X* direction, normalized with respect to the maximum value of each Hamming window, in order to highlight the main frequency content.

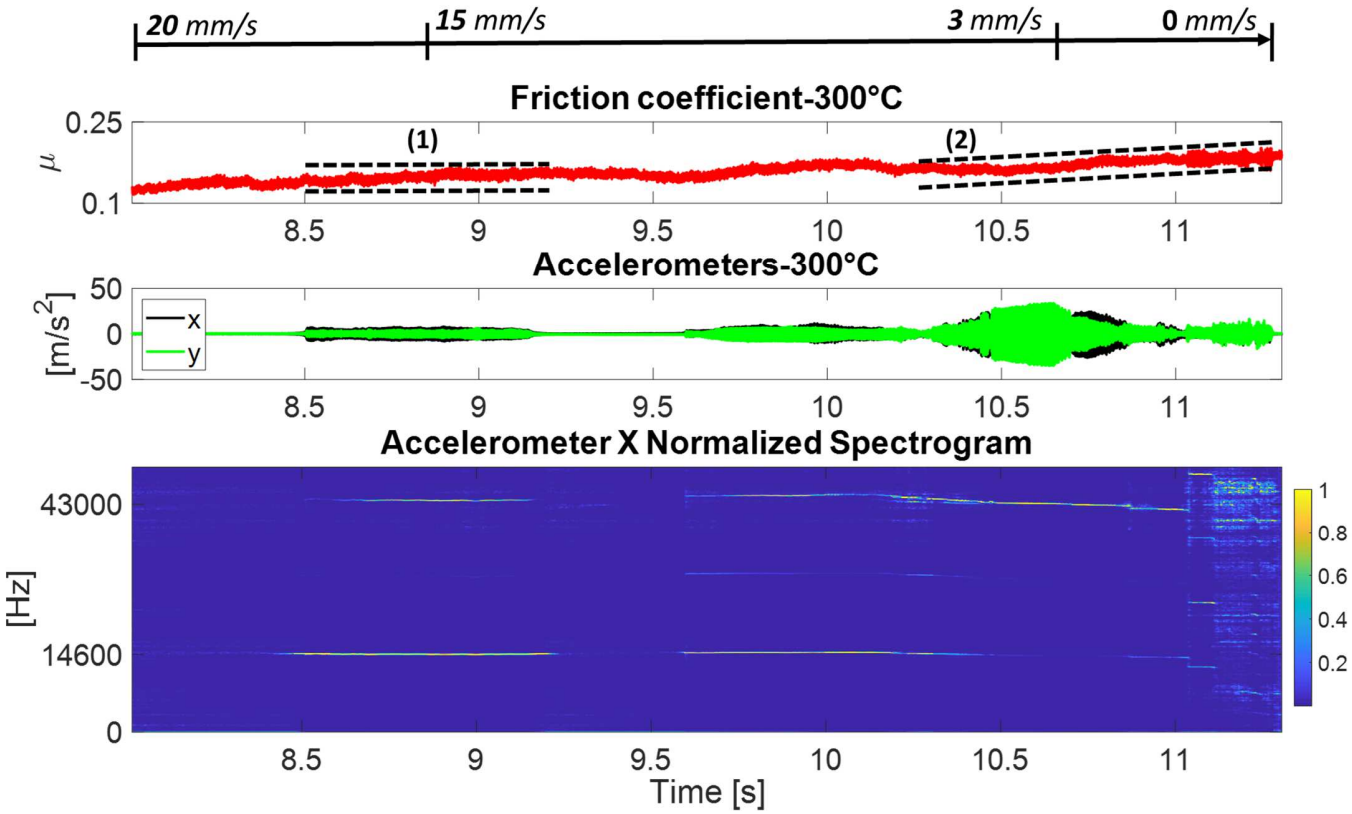

Figure 7. Example of signals recorded during a single stroke at 300 °C (third stroke of Figure 5) in the variable sliding velocity test (V=20⟶0 mm/s). From the top: friction coefficient, accelerometer signals along the tangential (X, black) and normal (Y, green) direction to the contact and normalized spectrogram of the acceleration along the X direction.

The scenario described in Figure 7 shows the occurrence of two different dynamic instabilities observed at different velocity ranges. The instabilities can be roughly distinguished, as a first attempt, thanks to the different amplitude and the different frequency content of the acceleration signals. A first dynamic

instability can be noticed at the beginning of braking, when the sliding velocity is still relatively high and the friction coefficient is almost constant (Figure 7, friction coefficient range (1)). From the spectrogram, it can be observed that the main frequency content is at almost 14.6 kHz. On the other hand, toward the end of braking, the friction coefficient is no longer constant and a sharp increase can be noticed (Figure 7, friction coefficient range (2)). Within this interval of decreasing velocity, where the friction coefficient is increasing (negative friction-velocity slope), the onset of a second dynamic instability can be observed. In this case, the main frequency content of almost 43 kHz can be detected by the spectrogram, pointing out a different unstable mode.

Meaningful information on the origin of the detected unstable friction-induced vibrations can be retrieved by investigating in further detail the vibrational response of the C/C specimens in both the tangential and normal directions to the contact. Figure 8 shows magnifications of the vibrational response along the *X* and *Y* directions of both the first instability (Figure 8.1), detected at a sliding velocity of almost 15 mm/s, and the second instability (Figure 8.2), detected at almost 3 mm/s.

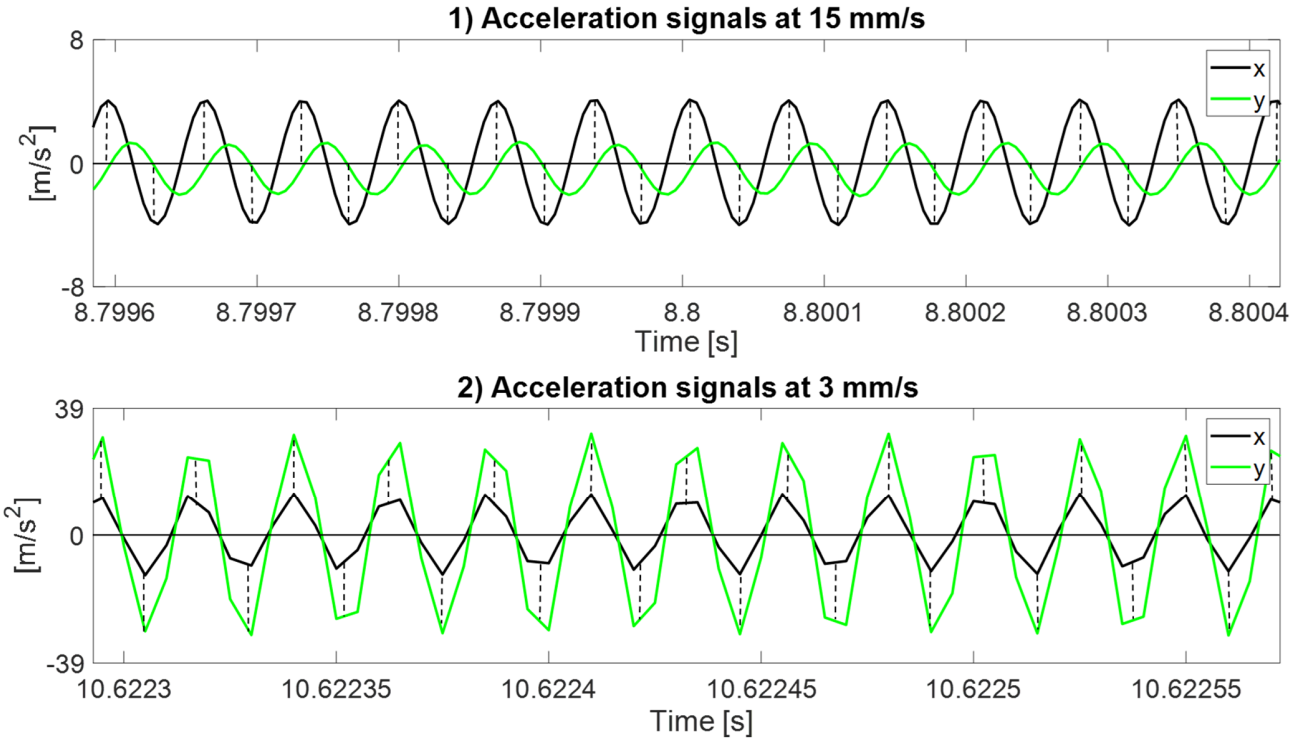

Figure 8. Detail of the vibrational response along the tangential (X) and normal (Y) directions for the mode coupling instability (1) and the negative friction-velocity slope (2) observed in Figure 7 at almost 15 mm/s and 3 mm/s, respectively.

In Figure 8.1, the vibrational response has been filtered by means of a low pass filter with a cutoff frequency of 20 kHz, in order to focus on the main frequency content of the mode coupling. During this first contact instability, it can be noticed that the vibrational signals recorded in the tangential (*X*) and normal direction (*Y*) are phase-shifted by almost 90°. Vertical dashed lines highlight that the maximum amplitude of oscillation, in the *X* direction, is reached when the vibrational signal in the *Y* direction is almost equal to zero, meaning that the signals are out of phase by almost 90°.

This is a typical feature retrieved in literature [45, 59-62] when dealing with squeal and mode coupling instability. The coupling of two modes of vibrations brings to the establishment of a phase shift of about 90° between the tangential and normal directions to the contact [45, 61, 62]. Then, the observed shift in

phase, brings to the assumption that the contact instability, observed within this range of velocities, where the friction is almost constant, is due to mode coupling.

On the other hand, Figure 8.2 shows that, during the instability at lower velocities, the vibrational signals, along the *X* and *Y* directions, are in phase. Vertical dashed lines show that the maximum amplitude of oscillation, in the *X* direction, is reached when the vibrational signal in the *Y* direction reaches its maximum as well, meaning that signals are in phase.

This is well correlated with the trend of the friction coefficient, which shows a negative friction-velocity slope and which brings a single mode of the system to be unstable, explaining the in-phase behavior of the tangential and normal components of the acceleration.

This outcome provides a direct tool for distinguishing the two different types of dynamic instabilities and allows for a better characterization of the main features of the unstable vibrational response of C/C materials at high-temperature condition.

To investigate further the observed phenomena, decoupling the effect of the imposed velocity variation, tests at constant velocity have been carried out at 15 mm/s and 3 mm/s, with the purpose of studying the main features of the instabilities originated by mode coupling and negative friction-velocity slope, respectively.

3.3 Result discussion: Constant velocity tests

The occurrence of the mode coupling instability has been then reproduced through a test performed at a constant sliding velocity of 15 mm/s, following the same temperature profile already described in Figure 3. As an example, Figure 9 shows the behavior of the friction coefficient and the vibrational response on both *X* and *Y* directions for two cycles of sliding motion at 300 °C and constant sliding velocity.

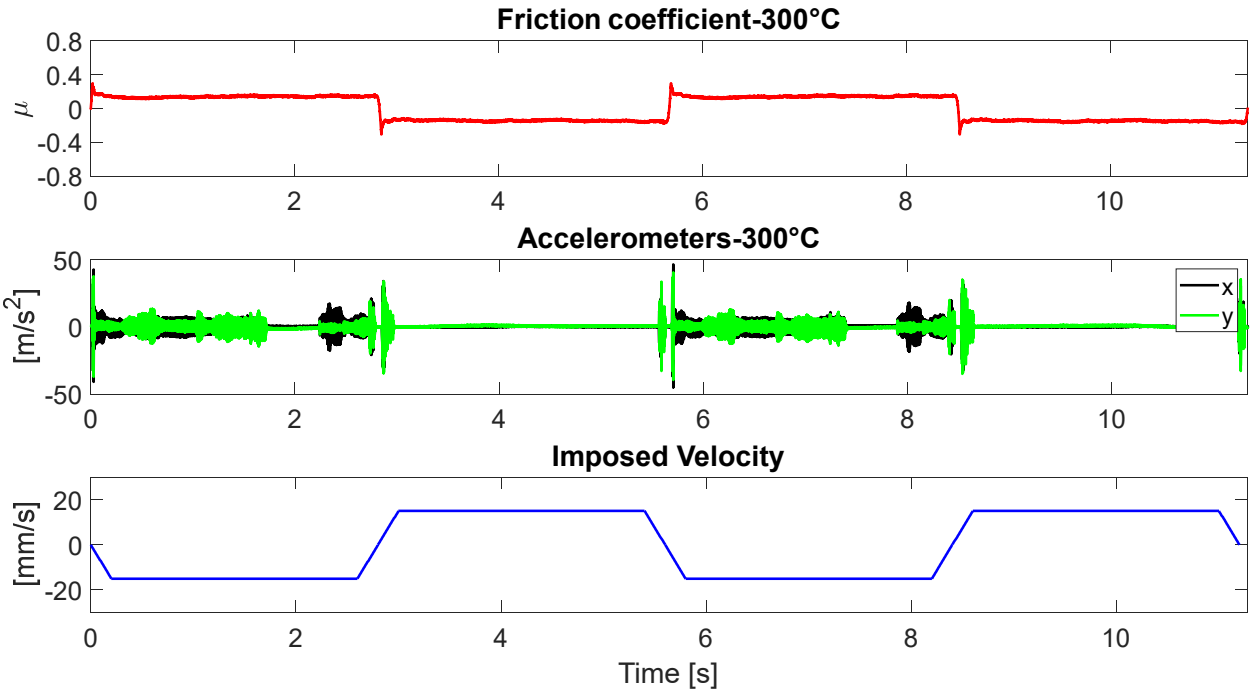

Figure 9. Example of signals recorded during two back-and-forth cycles, at 300 °C, in a constant sliding velocity test (V=15 mm/s). From the top: friction coefficient, accelerometer signals along the tangential (X, black) and normal (Y, green) direction to the contact and imposed sliding velocity profile.

An almost constant friction coefficient in each stroke and the occurrence of unstable friction-induced vibrations can be observed in Figure 9. Further information on the main features of the dynamic instability, arising under a constant sliding velocity equal to 15 mm/s, can be retrieved by investigating the vibrational response along the *X* and *Y* directions in a single stroke. Figure 10 shows a detail of the frictional and vibrational response of the third stroke of Figure 9.

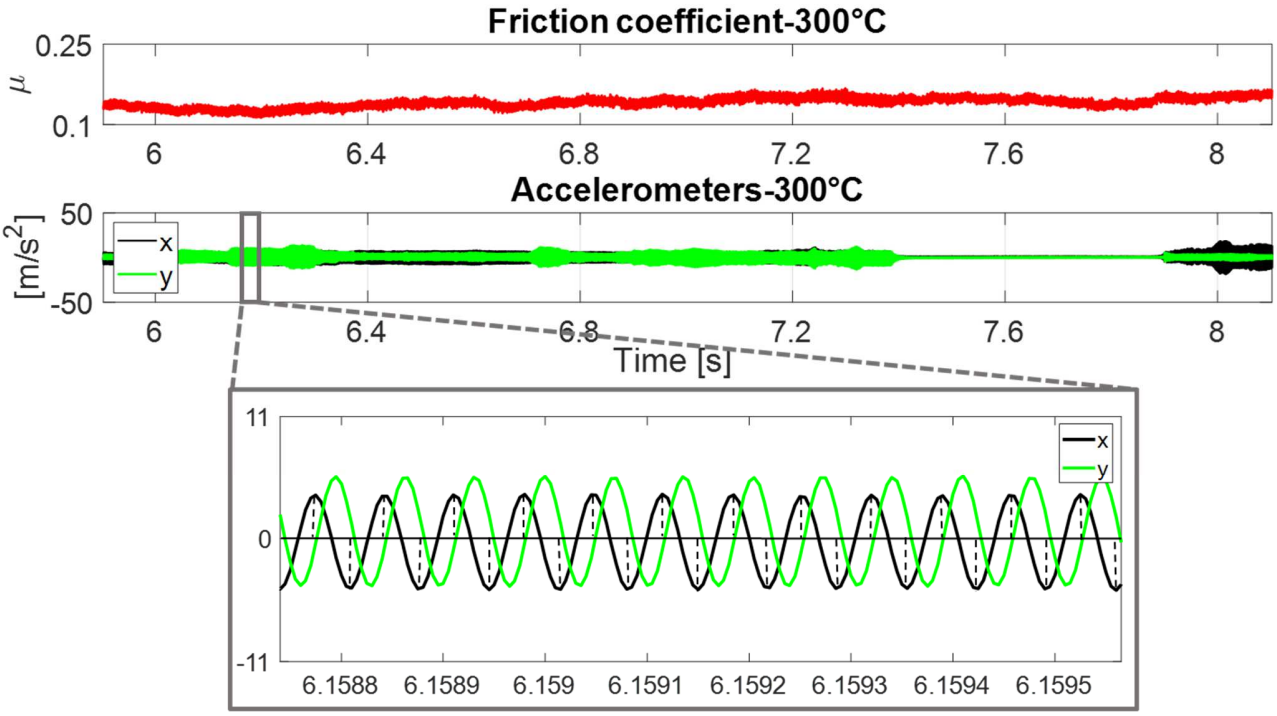

Figure 10. Detail of the friction coefficient and vibrational response of the third stroke of Figure 9. From the top: friction coefficient and accelerometer signals along the tangential (X) and normal (Y) direction to the contact.

Consistently with the dynamic instability observed during the braking test at almost 15 mm/s (Figure 8.1), also at constant velocity the onset of unstable friction-induced vibration is characterized by a phase shift of almost 90° between the *X* and *Y* direction, as shown in the zoom of Figure 10. Moreover, the main frequency content of the instability is almost 14.6 kHz, such as the one observed at 15 mm/s for the variable velocity test. The main features of the measured signals confirm the occurrence of a mode coupling instability.

A different scenario is the one retrieved under a constant sliding velocity equal to 3 mm/s. This test has been carried out in order to investigate the instability that arises in the range of sliding velocities where a negative friction-velocity slope is observed (detail (2) in Figure 7). In this range, the friction coefficient is no longer constant and, during the system vibration, an increase in the sliding velocity brings to a

decrease of the friction coefficient. Figure 11 shows, as an example, the behavior of the friction coefficient as well as the vibrational response of a single stroke at 300 °C.

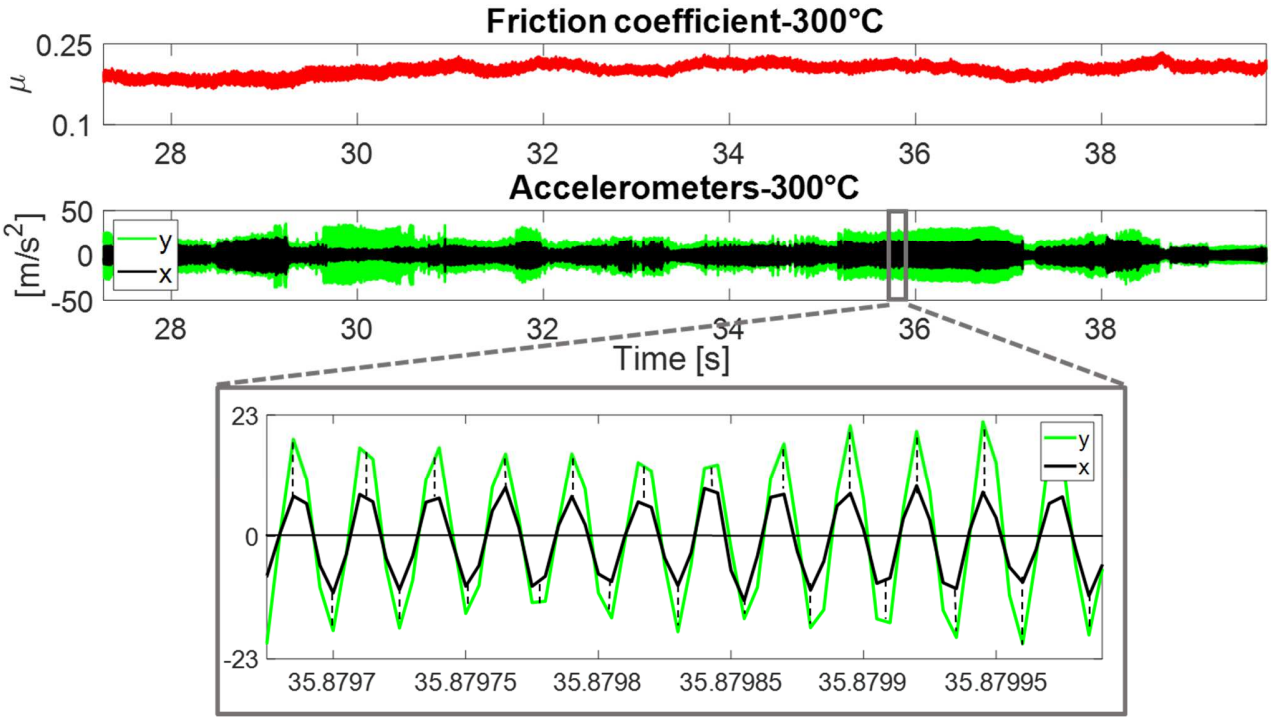

Figure 11. Detail of the friction coefficient and vibrational response of a single stroke at 300°C and in the constant sliding velocity test (V=3 mm/s). From the top: friction coefficient and accelerometer signals along the tangential (X) and normal (Y) direction to the contact.

Unstable friction-induced vibrations are observed during the whole stroke. Moreover, as can be seen from the zoom of Figure 11, in this case, the vibrational response is characterized by a higher frequency (almost 43 kHz), with respect to the mode coupling instability observed in Figure 10, and the acceleration signals along the tangential (*X*) and normal (*Y*) direction to the contact are in phase. This is consistent with the negative friction-velocity slope instability observed during the braking test (Figure 8.2), within the same velocity range, where the oscillation of the sliding velocity (i.e. of the friction coefficient) brings to modal instability .

In order to confirm the different origin of the observed instabilities (either mode coupling or negative friction-velocity slope), a numerical analysis has been developed to correlate the observed features of the vibrational signals with the measured trends of the friction coefficient.

4. Numerical analysis

A numerical investigation of the mode coupling and negative friction-velocity slope instabilities, characterizing the dynamic response of C/C materials, has been carried out by means of a two degrees-of-freedom lumped-parameter model. The analysis has been carried out by decoupling the onset of the two different kinds of unstable friction-induced vibrations in order to study the main features of the vibrational response when either a mode coupling or a negative friction-velocity slope instability occurs.

4.1 Lumped-parameter numerical model

The analyzed model consists of two masses, one of which is in frictional contact with a rigid translating plane. Consistently with the existing literature, the presence of two masses allows accounting for both the dynamics at the contact and that of the bulk of the mechanical system, providing a tool for simulating the vibrational response of a frictional system [46]. Figure 12 shows a diagram of the developed model.

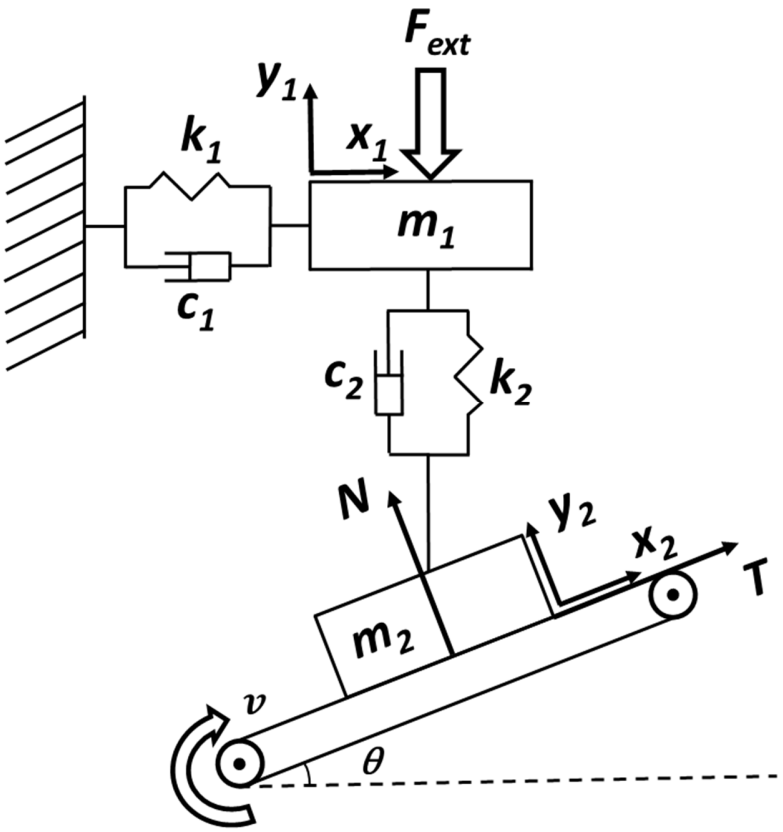

Figure 12. Diagram of the lumped-parameter model.

As shown in Figure 12, the mass m_2 is in frictional contact with a slider, inclined by an angle θ with respect to the horizontal plane and moving at a velocity v. The stiffness coefficients are indicated as k_1 and k_2 while the damping coefficients are referred to as c_1 and c_2. In the model, a preload is applied by means of an external force F_{ext}. The mass m_1 moves along the coordinates x_1 and y_1, while the motion of the mass m_2 is along the x_2 and y_2 directions. Moreover, the reaction force N, at the contact interface, between the mass m_2 and the slider, gives rise to a tangential force $T = \mu N$, where μ is the friction coefficient. In order to achieve a 2 DoF system, two constrains have been considered. The first condition imposes $y_2 = 0$, preventing the detachment of the mass m_2 from the slider. The second constraint equation

requires the coincidence between the horizontal motion of the mass m_1 and m_2 and it can be expressed as $x_1 = x_2 cos\theta$. Then, the equations of motion describing the numerical model can be written as follows:

$$M\underline{\ddot{r}} + C\underline{\dot{r}} + K\underline{r} = \underline{F} \tag{1}$$

Where:

$$M = \begin{bmatrix} m_1\, cos^2\,\theta + m_2 + \mu m_1 cos\theta sin\theta & 0 \\ 0 & m_1 \end{bmatrix} \tag{2}$$

$$C = \begin{bmatrix} c_1\, cos^2\,\theta + c_2\, sin^2\,\theta - \mu(c_2 - c_1) sin\theta cos\theta & c_2(\mu cos\theta - sin\theta) \\ -c_2 sin\theta & c_2 \end{bmatrix} \tag{3}$$

$$K = \begin{bmatrix} k_1\, cos^2\,\theta + k_2\, sin^2\,\theta - \mu(k_2 - k_1) sin\theta cos\theta & k_2(\mu cos\theta - sin\theta) \\ -k_2 sin\theta & k_2 \end{bmatrix} \tag{4}$$

$$\underline{F} = \begin{pmatrix} 0 \\ -F_{ext} \end{pmatrix} \tag{5}$$

$$\underline{r} = \begin{pmatrix} X \\ Y \end{pmatrix} \tag{6}$$

In particular, X and Y represent respectively x_2 and y_1, which are the two degrees of freedom of the numerical model. The values of the parameters introduced for the numerical analysis are reported in Table 2.

Parameter	Value
m_1	0.53 [kg]
m_2	0.045 [kg]
k_1	100000 [N/m]
k_2	101000 [N/m]
c_1	0.1 [kg/s]
c_2	0.1 [kg/s]
F_{ext}	100 [N]
θ	0.01 rad

Table 2. Parameters used in the numerical model for the analysis.

The parameters used in the numerical model have been selected with the aim of reproducing qualitatively the occurrence of the dynamic instabilities observed experimentally (i.e. mode coupling and negative-friction velocity slope) and retrieving the investigated features. The lumped model is not intended to quantitatively simulate the complex dynamics of the real frictional system.

It should be noticed that the significantly low value of θ allows considering the two degrees of freedom x_2 and y_1 as almost orthogonal. It is, therefore, reasonable to assume the vibrational response along X and Y as the vibrational components tangential and normal to the contact, respectively. As specified in the following sections, different trends of the friction coefficient μ, with respect to the sliding velocity, have been introduced in order to decouple the onset of mode coupling and negative friction-velocity slope instabilities, as observed experimentally. First, a complex eigenvalue analysis (CEA) has been carried out, as a function of μ, in order to characterize the dynamic response of the system.

4.2 Complex eigenvalue analysis

By computing the eigenvalues of the mechanical system, it is possible to predict the critical values of the friction coefficient leading to the occurrence of a mode coupling instability. The eigenvalues of a mechanical system characterized by a friction coefficient different from zero (asymmetric system matrices) can be found expressing the problem in the state space, as shown below:

$$\begin{cases} M\dot{\underline{r}} - M\underline{r} = 0 \\ M\ddot{\underline{r}} + C\dot{\underline{r}} + K\underline{r} = \underline{F} \end{cases} \tag{7}$$

That can be written as:

$$A\dot{\underline{p}} + B\underline{p} = \underline{Q} \tag{8}$$

Where:

$$A = \begin{bmatrix} 0 & M \\ M & C \end{bmatrix}, \; B = \begin{bmatrix} -M & 0 \\ 0 & K \end{bmatrix}, \; \underline{p} = \begin{bmatrix} \dot{\underline{r}} \\ \underline{r} \end{bmatrix} \text{ and } \underline{Q} = \begin{bmatrix} 0 \\ \underline{F} \end{bmatrix} \tag{9}$$

The eigenvalues of this numerical model can be written as follow:

$$\lambda_i = -\omega_i\delta_i \pm j\omega_i\sqrt{1-\delta_i^2} \tag{10}$$

Where ω_i is the angular frequency while δ_i is the modal damping factor. The value of the friction coefficient affects significantly the stability of the system, as it can be responsible for a negative modal damping factor and, therefore, a positive real part of the eigenvalues [33, 46, 47]. Such a condition leads to the onset of unstable friction-induced vibrations. In this respect, a value of μ higher than a specific threshold, depending on the parameters of the mechanical system, can lead to a mode coupling instability, where two different frequencies of the system coalesce together (lock-in) resulting in an unstable dynamical response [19, 40]. As an example, Figure 13 shows the complex eigenvalue analysis carried out as a function of the friction coefficient for the presented model.

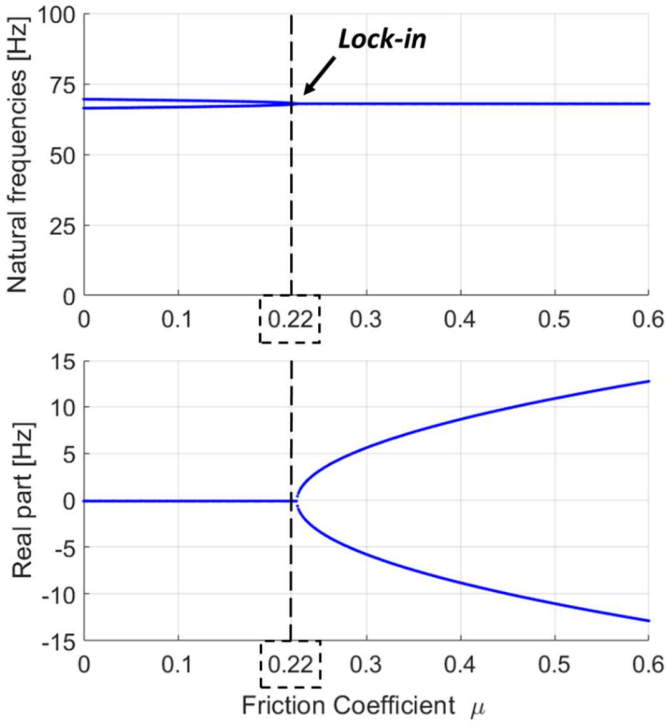

Figure 13. Real part and imaginary part (natural frequencies) of the eigenvalues as a function of the friction coefficient.

For a friction coefficient lower than 0.22, two separate modes of the system, characterized by different natural frequencies and positive damping, can be observed. As shown in Figure 13, the occurrence of a mode coupling instability arises for values of the friction coefficient higher than 0.22, where the initially separated frequencies merge together and one of the two real parts of the eigenvalues becomes positive (unstable mode). As a result, in order to study the vibrational response related to the mode coupling, for transient simulations, a constant friction coefficient equal to 0.5 will be imposed. Being greater than 0.22, such a value of μ is in the range of friction coefficient where a positive real part of the eigenvalues can be observed and, therefore, a mode coupling dynamic instability is expected to occur. On the other hand, an increasing μ from 0.05 to 0.15, while decreasing the relative velocity at the contact, will be imposed for simulating the onset of unstable friction-induced vibrations due to the negative friction-velocity

gradient. Being in a range of friction coefficient lower than 0.22, the occurrence of unstable friction-induced vibrations during braking will be, in this case, not affected by the mode coupling phenomenon. In this manner, the numerical decoupling of the mode coupling instability from the negative friction-velocity slope instability, allow for their characterization separately. In the following paragraph, the main results achieved by the respective transient simulations are presented.

4.3 Transient analysis

The vibrational response for the two degrees of freedom frictional system has been investigated for both the mode coupling and the negative friction-velocity slope instability. The transient analysis has been performed using Matlab/Simulink©, with an ode23s solver and maximum and minimum step sizes equal to 10^{-4} s and 10^{-5} s, respectively. In order to simulate a braking condition, a variable velocity of the sliding belt has been imposed. In particular, the analysis has been carried out with a decreasing velocity of the slider from 7 m/s to 0 m/s and a deceleration equal to 1 m/s^2. According to the complex eigenvalue analysis described in 4.2, a constant friction coefficient equal to 0.5 has been chosen to study the onset of the mode coupling instability. Figure 14 shows the vibrational response, in terms of acceleration, along the tangential (*X*) and normal (*Y*) direction to the contact, when the mode coupling instability arises.

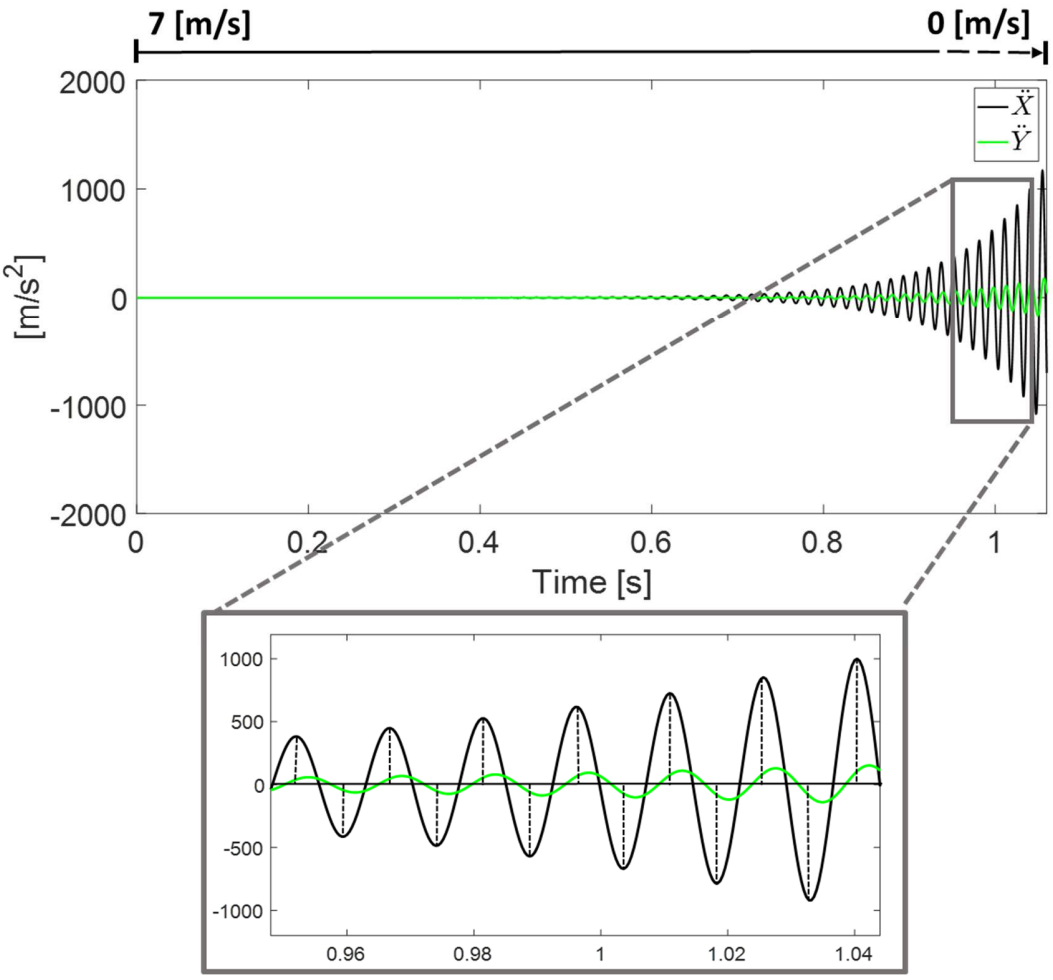

Figure 14. Onset of the mode coupling instability: acceleration $\ddot{X}$ and $\ddot{Y}$ with a constant friction coefficient equal to 0.5.

Consistently with the CEA, a constant friction coefficient higher than 0.22 leads to a mode coupling instability, with a frequency of the unstable mode equal to almost 68 Hz (Figure 13). The onset of the contact dynamic instability is characterized by an exponential increase in the amplitude of oscillation. Moreover, as can be seen from the zoom of Figure 14, the vibrational response along the X and Y directions shows a phase shift of the signals of almost 90°. This outcome is consistent with the experimental results related to the mode coupling instability, where a phase shift between the vibrational signals along the tangential and normal directions to the contact has been observed.

An analogous analysis has been also carried out, through the numerical model, on the negative friction-velocity slope instability. In this case, for the contact law at the contact interface between the mass m_2 and the slider, a linearly increasing friction coefficient with decreasing relative velocity has been imposed. Figure 15 shows the trend of the friction coefficient as a function of the relative velocity at the contact, defined as $\dot{X} - v$.

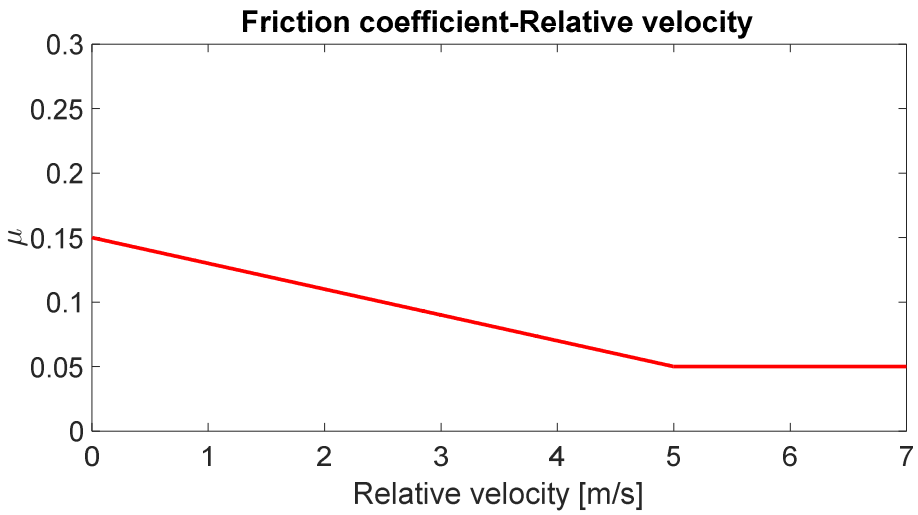

Figure 15. Friction coefficient vs relative velocity ($\dot{X} - v$) curve, implemented at the contact interface between the mass m_2 and the sliding belt.

In this case, the friction coefficient increases from 0.05 to 0.15, while decreasing the relative velocity from 5 m/s to 0 m/s. Being the friction coefficient lower than 0.22, the occurrence of a dynamic instability is only related to the negative friction-velocity gradient, because no mode coupling is observed (see Figure 13). The negative gradient leads to a negative apparent damping and consequently to an unstable dynamic response. The vibrational response in the X and Y directions, when the negative friction-velocity slope arises (exponential increase of the vibration amplitude), is shown in Figure 16.

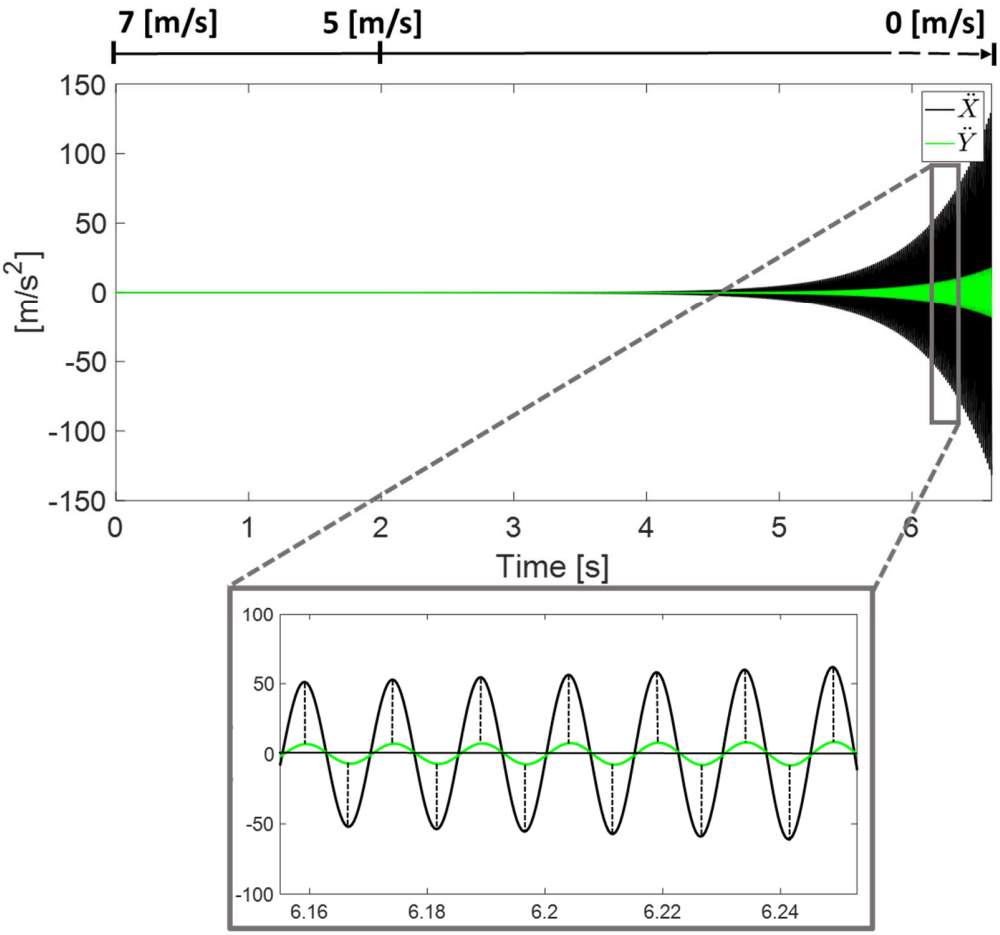

Figure 16. Onset of the negative friction-velocity slope instability: acceleration $\ddot{X}$ and $\ddot{Y}$ with a linearly increasing of the friction coefficient from 0.05 to 0.15 for a decreasing relative velocity from 5 m/s to 0 m/s.

The system is stable as long as the imposed velocity of the slider is higher than 5 m/s, being the friction coefficient constant in this range of sliding velocity. When the relative velocity decreases and becomes lower than 5 m/s, the system falls in the range of sliding velocities where the friction coefficient increases linearly according to the law described in Figure 15. In this velocity range, the negative friction-velocity slope at the contact interface leads to the occurrence of the dynamic instability, characterized by an exponential increase of the amplitude of vibration. As can be seen from the zoom of Figure 16, in this case, the unstable vibrational response is characterized by acceleration components, along the tangential

and normal direction to the contact, which are in phase. This result is coherent with the experimental outcome and highlights a specific feature of the negative friction-velocity slope instability, distinguishing it from the mode coupling, which is instead characterized by the phase shift, between the normal and tangential system response, of about 90°.

5. Conclusions

This paper presents a frictional and dynamic analysis on carbon-carbon material at a significantly high operative temperature condition (300 °C). The analysis of the contact dynamic instabilities, reproduced experimentally and simulated numerically, has provided meaningful information to distinguish the occurrence of a mode coupling instability from a negative friction-velocity slope instability.

The experimental characterization has been carried out through a specifically designed tribometer, consisting of air bearings in order to measure the frictional and vibrational response of the tested materials without any parasitic vibrations. A significantly different scenario from the room temperature condition and the 300 °C has been observed. While at 25 °C the friction coefficient is almost constant and no unstable friction-induced vibrations occur, at 300 °C the onset of unstable vibrational phenomena has been detected. The occurrence of the dynamic instabilities has been studied under both braking conditions (v = 20→0 mm/s) and constant sliding velocities (v = 15 mm/s and v = 3 mm/s). The experimental characterization highlighted the occurrence of a mode coupling instability at higher velocities, where the friction coefficient is almost constant, and the onset of a negative friction-velocity slope instability toward the end of braking, where the friction coefficient increases while decreasing the sliding velocity. By studying the main features of the two different dynamic instabilities, it has been observed a significant difference in the vibrational response along the tangential (X) and normal (Y) directions to the contact. While for the mode coupling instability the vibrational signals along the X and Y directions are out of

phase by almost 90°, for the negative friction-velocity slope instability the signals are in phase. The main features of the two different unstable friction-induced vibrations have been studied also numerically, thanks to a 2 DoF numerical model consisting of two masses, one of which in frictional contact with a sliding belt. A complex eigenvalue analysis, carried out as a function of the friction coefficient, has allowed decoupling the negative friction-velocity slope instability from the mode coupling and simulating the two phenomena separately. The obtained results are coherent with the experimental outcomes.

Overall, by one side, the obtained results allowed characterizing more in the detail the tribological and dynamic behavior of C/C composite materials. On the other side, by investigating the phase shift between tangential and normal accelerations to the contact, an effective tool is here proposed to distinguish the nature of the unstable friction-induced vibrations, which is of main interest for industrial applications. In fact, whenever frictional contact occurs, different contact instabilities can arise [9, 63], and identifying the origin of the encountered unstable vibrations can help in determining solutions for their suppression. As a next step, a finite element model of the experimental setup will be developed for a quantitative simulation of the investigated phenomena, by both complex eigenvalue analysis and transient nonlinear simulations.

6. Acknowledgments

A.L. acknowledges the French National Association of Research and Technology (ANRT) for its support to this work through the CIFRE convention N° 2018/1016.

F.M. acknowledges the Sapienza University of Rome for partially funding this study by the research project funding no. RM11916B4695CF24.

7. References

[1] E. Fitzer and L. M. Manocha, *Carbon reinforcements and carbon/carbon composites*. Springer Science & Business Media, 2012.

[2] D. Gadow and M. Jiménez, "Carbon fiber- reinforced carbon composites for aircraft brakes," *American Ceramic Society Bulletin,* vol. 98, pp. 28-34, 2019.

[3] G. R. Devi and K. R. Rao, "Carbon Carbon Composites: An Overview," *Defence Science Journal,* vol. 43, no. 4, p. 369, 1993.

[4] T. Windhorst and G. Blount, "Carbon-carbon composites: a summary of recent developments and applications," *Materials & Design,* vol. 18, no. 1, pp. 11-15, 1997.

[5] R. A. Ibrahim, "“Friction-Induced Vibration, Chatter, Squeal, and Chaos—Part I: Mechanics of Contact and Friction”," *Applied Mechanics Reviews,* vol. 47, no. 7, pp. 209–226, Jul. 1994.

[6] A. Akay, "Acoustics of friction," *The Journal of the Acoustical Society of America,* vol. 111, no. 4, pp. 1525-1548, 2002.

[7] A. Meziane, S. D'Errico, L. Baillet, and B. Laulagnet, "Instabilities generated by friction in a pad–disc system during the braking process," *Tribology International,* vol. 40, no. 7, pp. 1127-1136, 2007.

[8] F. Massi, Y. Berthier, and L. Baillet, "Contact surface topography and system dynamics of brake squeal," *Wear,* vol. 265, no. 11, pp. 1784-1792, 2008.

[9] D. Tonazzi, F. Massi, L. Baillet, A. Culla, M. Di Bartolomeo, and Y. Berthier, "Experimental and numerical analysis of frictional contact scenarios: from macro stick–slip to continuous sliding," *Meccanica,* vol. 50, no. 3, pp. 649-664, 2015.

[10] D. Tonazzi, F. Massi, A. Culla, L. Baillet, A. Fregolent, and Y. Berthier, "Instability scenarios between elastic media under frictional contact," *Mechanical Systems and Signal Processing,* vol. 40, no. 2, pp. 754-766, 2013.

[11] H. Ouyang, W. Nack, Y. Yuan, and F. Chen, "Numerical analysis of automotive disc brake squeal: a review," *International Journal of Vehicle Noise and Vibration,* vol. 1, no. 3-4, pp. 207-231, 2005.

[12] A. Meziane, L. Baillet, and B. Laulagnet, "Experimental and numerical investigation of friction-induced vibration of a beam-on-beam in contact with friction," *Applied Acoustics,* vol. 71, no. 9, pp. 843-853, 2010.

[13] N. S. Eiss, "Frictional Instabilities," Dordrecht, 1998: Springer Netherlands, in Tribology Issues and Opportunities in MEMS, pp. 149-156.

[14] D. Tonazzi, F. Massi, M. Salipante, L. Baillet, and Y. Berthier, "Estimation of the Normal Contact Stiffness for Frictional Interface in Sticking and Sliding Conditions," *Lubricants,* vol. 7, no. 7, 2019.

[15] Z. Li, H. Ouyang, and Z.-H. Wei, "Insights into instability of friction-induced vibration of multi-degree-of-freedom models," *Journal of Sound and Vibration,* vol. 503, 2021.

[16] D. W. Wang, J. L. Mo, Q. Zhang, J. Zhao, H. Ouyang, and Z. R. Zhou, "The effect of the grooved elastic damping component in reducing friction-induced vibration," *Tribology International,* vol. 110, pp. 264-277, 2017.
[17] H. H. Qian, J. L. Mo, Z. Y. Xiang, Z. Y. Fan, Y. K. Wu, and Z. R. Zhou, "The effect of the macroscopic surface morphology caused by the uneven wear on friction induced vibration," *Tribology International,* vol. 154, p. 106672, 2021.
[18] Y. K. Wu, B. Tang, Z. Y. Xiang, H. H. Qian, J. L. Mo, and Z. R. Zhou, "Brake squeal of a high-speed train for different friction block configurations," *Applied Acoustics,* vol. 171, 2021.
[19] M. North, *Disc brake squeal: a theoretical model*. MIRA Noneaton, 1972.
[20] A. Bajer, V. Belsky, and L. J. Zeng, "Combining a nonlinear static analysis and complex eigenvalue extraction in brake squeal simulation," SAE Technical Paper, 0148-7191, 2003.
[21] J. Kang, C. M. Krousgrill, and F. Sadeghi, "Comprehensive stability analysis of disc brake vibrations including gyroscopic, negative friction slope and mode-coupling mechanisms," *Journal of Sound and Vibration,* vol. 324, no. 1, pp. 387-407, 2009.
[22] I. Ghezzi, D. Tonazzi, M. Rovere, C. Le Coeur, Y. Berthier, and F. Massi, "Tribological investigation of a greased contact subjected to contact dynamic instability," *Tribology International,* vol. 143, p. 106085, 2020.
[23] I. Ghezzi, D. Tonazzi, M. Rovere, C. Le Coeur, Y. Berthier, and F. Massi, "Frictional behaviour of a greased contact under low sliding velocity condition," *Tribology International,* vol. 155, 2021.
[24] A. Lazzari, D. Tonazzi, and F. Massi, "Squeal propensity characterization of brake lining materials through friction noise measurements," *Mechanical Systems and Signal Processing,* vol. 128, pp. 216-228, 2019.
[25] B. Hervé, J. J. Sinou, H. Mahé, and L. Jézéquel, "Analysis of squeal noise and mode coupling instabilities including damping and gyroscopic effects," *European Journal of Mechanics - A/Solids,* vol. 27, no. 2, pp. 141-160, 2008.
[26] S. Oberst and J. C. S. Lai, "Nonlinear transient and chaotic interactions in disc brake squeal," *Journal of Sound and Vibration,* vol. 342, pp. 272-289, 2015.
[27] M. Stender, M. Tiedemann, L. Hoffmann, and N. Hoffmann, "Determining growth rates of instabilities from time-series vibration data: Methods and applications for brake squeal," *Mechanical Systems and Signal Processing,* vol. 129, pp. 250-264, 2019.
[28] H. Ouyang, J. E. Mottershead, M. P. Cartmell, and M. I. Friswell, " Friction-induced parametric resonances in discs: effect of a negative friction-velocity relationship," *Journal of Sound and Vibration,* vol. 209, no. 2, pp. 251-264, 1998.
[29] M. Di Bartolomeo, A. Lazzari, M. Stender, Y. Berthier, A. Saulot, and F. Massi, "Experimental observation of thermally-driven frictional instabilities on C/C materials," *Tribology International,* vol. 154, 2021.
[30] H. Mills, *Brake squeak*. Institution of Automobile Engineers, 1938.
[31] A. Papangelo, M. Ciavarella, and N. Hoffmann, "Subcritical bifurcation in a self-excited single-degree-of-freedom system with velocity weakening–strengthening friction law: analytical results and comparison with experiments," *Nonlinear Dynamics,* vol. 90, no. 3, pp. 2037-2046, 2017.
[32] G. X. Chen and Z. R. Zhou, "Correlation of a negative friction–velocity slope with squeal generation under reciprocating sliding conditions," *Wear, 14th International Conference on Wear of Materials,* vol. 255, no. 1, pp. 376-384, 2003.
[33] K. Shin, M. J. Brennan, J. E. Oh, and C. J. Harris, "Analysis of disc brake noise using a two-degree-of-freedom model," *Journal of Sound and Vibration,* vol. 254, no. 5, pp. 837-848, 2002.

[34] H. Hetzler, "On the effect of nonsmooth Coulomb friction on Hopf bifurcations in a 1-DoF oscillator with self-excitation due to negative damping," *Nonlinear Dynamics,* vol. 69, no. 1, pp. 601-614, 2012.
[35] A. Lazzari, D. Tonazzi, G. Conidi, C. Malmassari, A. Cerutti, and F. Massi, "Experimental Evaluation of Brake Pad Material Propensity to Stick-Slip and Groan Noise Emission," *Lubricants,* vol. 6, no. 4, 2018.
[36] P. Vielsack, "Stick–slip instability of decelerative sliding," *International Journal of Non-Linear Mechanics,* vol. 36, no. 2, pp. 237-247, 2001.
[37] J. J. Sinou, O. Dereure, G. B. Mazet, F. Thouverez, and L. Jezequel, "Friction-induced vibration for an aircraft brake system—Part 1: Experimental approach and stability analysis," vol. 48, no. 5, pp. 536-554, 2006.
[38] J. J. Sinou, F. Thouverez, L. Jezequel, O. Dereure, and G. B. Mazet, "Friction induced vibration for an aircraft brake system—Part 2: Non-linear dynamics," *International Journal of Mechanical Sciences,* vol. 48, no. 5, pp. 555-567, 2006.
[39] D. Tonazzi, F. Massi, L. Baillet, J. Brunetti, and Y. Berthier, "Interaction between contact behaviour and vibrational response for dry contact system," *Mechanical Systems and Signal Processing,* vol. 110, pp. 110-121, 2018.
[40] F. Massi, L. Baillet, O. Giannini, and A. Sestieri, "Brake squeal: Linear and nonlinear numerical approaches," *Mechanical Systems and Signal Processing,* vol. 21, no. 6, pp. 2374-2393, 2007.
[41] M. Stender, M. Di Bartolomeo, F. Massi, and N. Hoffmann, "Revealing transitions in friction-excited vibrations by nonlinear time-series analysis," *Nonlinear Dynamics,* vol. 98, no. 4, pp. 2613-2630, 2019.
[42] K. Popp, M. Rudolph, M. Kroger, and M. Lindner, "Mechanisms to generate and to avoid friction induced vibrations," *VDI BERICHTE,* vol. 1736, pp. 1-16, 2002.
[43] U. von Wagner, D. Hochlenert, and P. Hagedorn, "Minimal models for disk brake squeal," *Journal of Sound and Vibration,* vol. 302, no. 3, pp. 527-539, 2007.
[44] J.J. Sinou and L. Jézéquel, "Mode coupling instability in friction-induced vibrations and its dependency on system parameters including damping," *European Journal of Mechanics - A/Solids,* vol. 26, no. 1, pp. 106-122, 2007.
[45] N. Hoffmann, M. Fischer, R. Allgaier, and L. Gaul, "A minimal model for studying properties of the mode-coupling type instability in friction induced oscillations," *Mechanics Research Communications,* vol. 29, no. 4, pp. 197-205, 2002.
[46] J. Brunetti, F. Massi, W. D'Ambrogio, and Y. Berthier, "Dynamic and energy analysis of frictional contact instabilities on a lumped system," *Meccanica,* vol. 50, no. 3, pp. 633-647, 2015.
[47] N. Hoffmann and L. Gaul, "Effects of damping on mode-coupling instability in friction induced oscillations," *ZAMM-Journal of Applied Mathematics and Mechanics/Zeitschrift für Angewandte Mathematik und Mechanik: Applied Mathematics and Mechanics,* vol. 83, no. 8, pp. 524-534, 2003.
[48] M. Renouf, F. Massi, N. Fillot, and A. Saulot, "Numerical tribology of a dry contact," *Tribology International,* vol. 44, no. 7, pp. 834-844, 2011.
[49] A. R. AbuBakar and H. Ouyang, "A prediction methodology of disk brake squeal using complex eigenvalue analysis," *International Journal of Vehicle Design,* vol. 46, no. 4, pp. 416-435, 2008.
[50] L. Charroyer, O. Chiello and J. J. Sinou, "Parametric study of the mode coupling instability for a simple system with planar or rectilinear friction," *Journal of Sound and Vibration,* vol. 384, pp. 94-112.

[51] M. Di Bartolomeo, G. Lacerra, L. Baillet, E. Chatelet, F. Massi, "Parametrical experimental and numerical analysis on friction-induced vibrations by a simple frictional system," *Tribology International,* vol. 112, pp. 47-57.

[52] G. Lacerra, M. Di Bartolomeo, S. Milana, L. Baillet, E. Chatelet, and F. Massi, "Validation of a new frictional law for simulating friction-induced vibrations of rough surfaces," *Tribology International,* vol. 121, pp. 468-480, 2018.

[53] J. R. Gomes, O. M. Silva, C. M. Silva, L. C. Pardini, and R. F. Silva, "The effect of sliding speed and temperature on the tribological behaviour of carbon–carbon composites," *Wear- Proceedings of the ninth Nordic Symposium on Tribology,* vol. 249, no. 3, pp. 240-245, 2001.

[54] J. Y. Paris, L. Vincent, and J. Denape, "High-speed tribological behaviour of a carbon/silicon-carbide composite," *Composites Science and Technology,* vol. 61, no. 3, pp. 417-423, 2001.

[55] Y. Waddad, V. Magnier, P. Dufrénoy, and G. De Saxcé, "Multiscale thermomechanical modeling of frictional contact problems considering wear – Application to a pin-on-disc system," *Wear,* vol. 426-427, pp. 1399-1409, 2019.

[56] R. Mann, V. Magnier, J. F. Brunel, P. Dufrénoy, M. Henrion, and E. Guillet-Revol, "Thermomechanical characterization of high-speed train braking materials to improve models: Numerical validation via a comparison with an experimental braking test," *Tribology International,* vol. 156, 2021.

[57] H. Kasem, S. Bonnamy, Y. Berthier, P. Dufrénoy, and P. Jacquemard, "Tribological, physicochemical and thermal study of the abrupt friction transition during carbon/carbon composite friction," *Wear,* vol. 267, no. 5, pp. 846-852, 2009.

[58] M. Gouider, Y. Berthier, P. Jacquemard, B. Rousseau, S. Bonnamy, and H. Estrade-Szwarckopf, "Mass spectrometry during C/C composite friction : carbon oxidation associated with high friction coefficient and high wear rate," (in French), *Wear,* pp. 1082-1087, 2004 2004.

[59] B. Ding, G. Squicciarini, D. Thompson, and R. Corradi, "An assessment of mode-coupling and falling-friction mechanisms in railway curve squeal through a simplified approach," *Journal of Sound and Vibration,* vol. 423, pp. 126-140, 2018.

[60] F. Massi, O. Giannini, and L. Baillet, "Brake squeal as dynamic instability: an experimental investigation," *The Journal of the Acoustical Society of America,* vol. 120, no. 3, pp. 1388-1398, 2006.

[61] O. Giannini, A. Akay, and F. Massi, "Experimental analysis of brake squeal noise on a laboratory brake setup," *Journal of Sound and Vibration,* vol. 292, no. 1, pp. 1-20, 2006.

[62] A. Akay, O. Giannini, F. Massi, and A. Sestieri, "Disc brake squeal characterization through simplified test rigs," *Mechanical systems and signal processing,* vol. 23, no. 8, pp. 2590-2607, 2009.

[63] D. Tonazzi, F. Massi, A. Culla, L. Baillet, A. Fregolent and Y. Berthier, "Instability scenarios betweenelastic media under frictional contact," *Mechanical Systems and Signal Processing,* vol. vol. 40, no. 2, pp. pp. 754–766, Nov. 2013.